



13th International Conference on Greenhouse Gas Control Technologies, GHGT-13, 14-18  
November 2016, Lausanne, Switzerland

## Closing of micro-cavities in well cement upon exposure to CO<sub>2</sub> brine

E.A. Chavez Panduro<sup>a</sup>, M. Torsæter<sup>b\*</sup>, K. Gawel<sup>b</sup>, R. Bjørge<sup>c</sup>, A. Gibaud<sup>d</sup>, Y. Yang<sup>e</sup>, H. O. Sørensen<sup>e</sup>, P. Frykman<sup>f</sup>, C. Kjøller<sup>f</sup>, D. W. Breiby<sup>a</sup>

<sup>a</sup>Department of Physics, Norwegian University of Science and Technology (NTNU), Høgskoleringen 5, 7491 Trondheim, Norway

<sup>b</sup>SINTEF Petroleum Research, Trondheim, Norway

<sup>c</sup>SINTEF Materials and Chemistry, Trondheim, Norway

<sup>d</sup>LUMAN, IMMM, UMR 6283 CNRS, Université du Maine, Le Mans Cedex 09, France

<sup>e</sup>University of Copenhagen, Department of Chemistry, Copenhagen, Denmark

<sup>f</sup>Geological Survey of Denmark and Greenland, Copenhagen, Denmark

### Abstract

Long-lasting cement plugging of wells is crucial for successful CO<sub>2</sub> storage in underground reservoirs. It requires a profoundly improved understanding of the behavior of fractured cement under realistic subsurface conditions including elevated temperature, high pressure and the presence of CO<sub>2</sub> saturated brine. Here we report computed X-ray tomography studies on the effects of CO<sub>2</sub> on cement. More specifically, we have exposed cured Portland G cement samples with pre-made microchannels mimicking fractures to CO<sub>2</sub> saturated brine at elevated pressure (100 bars) and room temperature. The microchannels were observed to get filled with calcite (CaCO<sub>3</sub>) during the CO<sub>2</sub> exposure. The extent of this self-healing was dependent on the diameter of the leakage path, with narrower channels more readily getting clogged. Chemical simulations taking into account the cement composition, CO<sub>2</sub> availability, pH, pressure and temperature gave results consistent with our conceptual understanding of how the differences in dissolution/precipitation profiles in the cement may result from the availability of CO<sub>2</sub>. In particular, the modelling provides an explanation why calcite precipitates preferentially in the channels rather than on the external cement sample surfaces. We conclude that the localized precipitation can be ascribed to higher pH inside the cavities compared to near the external surfaces, owing to long diffusion distances giving a locally limited CO<sub>2</sub> supply within the voids.

© 2017 The Authors. Published by Elsevier Ltd. This is an open access article under the CC BY-NC-ND license (<http://creativecommons.org/licenses/by-nc-nd/4.0/>).

Peer-review under responsibility of the organizing committee of GHGT-13.

**Keywords:** CO<sub>2</sub>, cement, self-healing, microcomputed tomography

\* Corresponding author. Tel: +47 4811-1159

E-mail address: [malin.torsater@sinetf.no](mailto:malin.torsater@sinetf.no)

## 1. Introduction

CO<sub>2</sub> Capture and Storage (CCS) using depleted oil and gas reservoirs is considered a promising solution for reducing global emissions of greenhouse gases but large-scale implementation is impeded by a fear of CO<sub>2</sub> leakage from the reservoirs[1]. The special report on CCS published by the Intergovernmental Panel of Climate Change (IPCC) outlines that wells are among the most probable leakage paths from CO<sub>2</sub> storage sites[1]. These wells are man-made structures of steel and cement that connect the storage reservoir with the atmosphere. If the steel or cement barriers break, leakage paths are likely to develop along the well. To estimate potential leakage rates over time, and to optimize well remediation protocols, the compatibility of Portland cement with CO<sub>2</sub> has been studied through several experimental campaigns[2–5].

When it comes to CO<sub>2</sub> exposure of cement, an important finding is that in addition to the critical fact that cement tends to get more brittle at the surface when carbonated, fractures in samples have been observed to heal - which is clearly promising[3,4]. Self-healing has been observed both at hydrostatic non-flow ("batch") conditions and CO<sub>2</sub> flow conditions. At non-flow conditions, where a sample is immersed in a CO<sub>2</sub>-rich aqueous environment, a decrease of the porosity and permeability has been observed in artificially fractured cement bars[6]. Similar effects have been observed when CO<sub>2</sub> has been flowed through fractured samples, and the permeability decrease can in this case be ascribed to carbonation inside cracks[7,8]. It has been found that the chemical changes occurring in the samples are not the same in batch conditions and CO<sub>2</sub> flow conditions[9,10]. In the former case, the self-healing occurs by CaCO<sub>3</sub> precipitation but in the latter case the cement degrades into an amorphous layer on the fracture surfaces leading to a decrease of the permeability. In order to make use of this beneficial cement healing process in practice, a more detailed understanding is required of how it occurs and how it affects CO<sub>2</sub> leakage rates. To elucidate these issues, we have performed micro-computed tomography ( $\mu$ -CT) experiments on artificially fractured cement to observe the healing process as well as the carbonation process at batch conditions. We have exposed cement samples with pre-made microchannels (mimicking defects) to CO<sub>2</sub> at high pressure. The experiments have been performed at 100 bars pressure and room temperature. The experiments were supplemented by modelling of compositional changes both within the cement sample as well as in the solution. The models have been set up in order to understand possible differences in dissolution profiles in the cement that may result from the availability of CO<sub>2</sub>.

## 2. Experimental

### 2.1. Sample preparation

Portland G cement (High Sulfate Resistant Well Cement, Norcem AS) was mixed according to API recommended practice[11] with a water/cement ratio mass of 0.44. The slurry was poured into cylindrical plastic moulds of diameter 3 mm. Nylon fishing lines ( $\phi = 0.2$  and 0.5 mm) were inserted into the cement slurry in order to form channels in the samples. The samples were cured for 3 days at ambient temperature and pressure. Then both moulds and fishing lines were carefully removed, thereby leaving a cylindrical cavity running through the free-standing sample. The samples were left for further curing in plastic bags to avoid water evaporation and drying. The curing lasted for two weeks before CO<sub>2</sub> exposure.

### 2.2. CO<sub>2</sub> exposure and X-ray microtomography

The experiments were performed at 100 bars and room temperature at batch conditions in a small pressure cell dedicated for in-situ CT studies. The pressure cell was equipped with a sample holder with an inner diameter of 4 mm and  $\sim 1$  cm<sup>3</sup> in volume. The batch aqueous solution contained 1 wt% of NaCl. The hydrostatic pressure was increased up to 100 bars within 2 hours and maintained for 2 hours at room temperature. The pressure was lowered from 100 bars back to ambient over 30 minutes.

The  $\mu$ -CTs images of cement sample during the CO<sub>2</sub> exposure were collected using a Nikon XT H225  $\mu$ -CT at 145 keV and 87  $\mu$ A at the Department of Physics, NTNU. Each tomogram was reconstructed from 3142 projections collected over 360 degree rotation and with an exposure time of 2 s for each projection. The reconstructed 3D tomogram had a resolution of about 10  $\mu$ m (voxel size of 3.8  $\mu$ m) using the CTAgent software.

Image visualization and segmentation were carried out using VGstudio and Fiji[12] software. Segmentation of the carbonated zones and the precipitated calcium carbonate from the  $\mu$ -CT image was done under the assumption that the calcium carbonate containing layer is denser, and therefore brighter and more homogeneous in the (inverted)  $\mu$ -CT images. The mineral precipitation was segmented by using a threshold of the gray-scale histogram in the microcavity section.

### 2.3. Modelling

Reactive geochemical modelling was carried out using the numerical code PHREEQC[13] with the Thermoddem database[14] in order to be able to represent the cement in the model. In order to simulate chemical reactions taking place at the water/cement interface, two 1D transport models were set up. In both cases, the numerical grid represented a cross-section across the interface, i.e. the water/cement interface was present at one end of the model while the other end represented the interior of the cement. At the cement end of the model grid, the boundary was simulated as a closed boundary (Neumann boundary condition) while at the interface end of the model grid, the boundary condition varied in the two conceptual models. In one model, the boundary condition was of Dirichlet type (open boundary) obtained by keeping the water in equilibrium with a constant CO<sub>2</sub> pressure of 50 bars in order to model a situation with unlimited supply of CO<sub>2</sub> to the water phase. In the second model, the boundary condition was of Neumann type (closed boundary) but with an initial concentration of CO<sub>2</sub> in the water corresponding to equilibrium with a CO<sub>2</sub> pressure of 50 bars to model the limited supply of CO<sub>2</sub>. Except for the different boundary conditions at the water/cement interface, the two conceptual models were similar.

The numerical grid was represented by a 1D column with 25 cells, each 0.1 mm long, of which five cells at one end represented the water phase. Transport was simulated as diffusion only since the permeability of the cement is assumed to be very low. The diffusion coefficient for CO<sub>2</sub> was set to  $1.6 \times 10^{-9}$  m<sup>2</sup>/s which is line with Cadogan et al.[15].

The cement was represented as a simple cement consisting of calcium-silica-hydrate (C-S-H(1.6)) and portlandite (Ca(OH)<sub>2</sub>), and the relative amounts of these minerals initially present in the cement were taken from Soive et al.[16]. As a consequence of the reactions between CO<sub>2</sub> and cement, calcite (CaCO<sub>3</sub>) was allowed to precipitate in the model, but was not considered to be present in the sample initially. The models simulated a total of 275 min of reactive transport by 400 time steps, each 126 sec long.

## 3. Results and discussion

CO<sub>2</sub> exposure of Portland G cement cylinders ( $\phi \sim 3$  mm) containing one through-going microcavity ( $\phi \sim 0.2$  and 0.5 mm) were studied using  $\mu$ -CT. The samples were immersed in brine solution and then exposed to CO<sub>2</sub> at 100 bars for 20 hours. After the CO<sub>2</sub> exposure at batch conditions, mineral precipitation in the micro-cavities was observed. Figure 1 shows the cross-sections through cement samples before and after exposure. Micro-cavities of both cement samples were partially filled with precipitate after exposure to CO<sub>2</sub> saturated brine. The precipitate was calcium carbonate (CaCO<sub>3</sub>), and X-ray diffraction on the exposed samples indicated that the polymorph was calcite. The CaCO<sub>3</sub> crystals were randomly located along the cavity surface. After 20 h the mineral occupied about 40 % and 22 % of the 0.2 mm and 0.5 mm diameter microcavities, respectively. Notably, no precipitate was observed at the external sample surfaces being in contact with large solvent volumes.

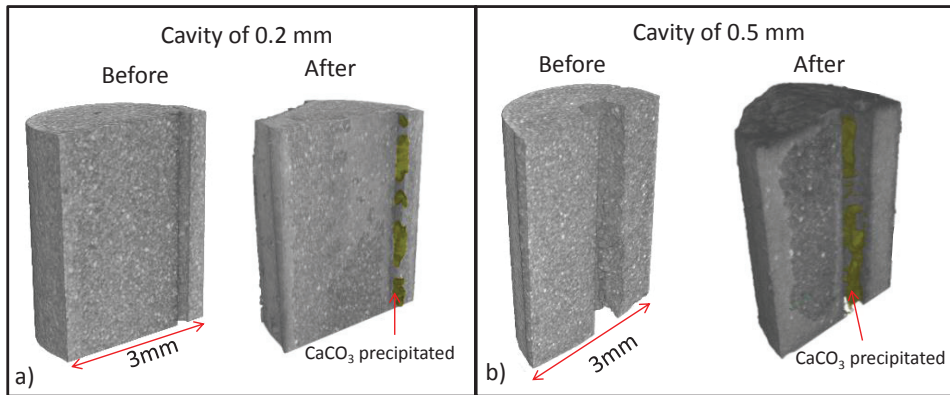


Fig. 1. Vertical cross-sections through micro computed tomography ( $\mu$ -CT) reconstructed volumes for samples with a) 0.2 mm and b) 0.5 mm void diameters before and after  $\text{CO}_2$  exposure.  $\text{CaCO}_3$  was found to precipitate inside, and thereby nearly close, the voids, while no precipitates was found on the external sample surfaces.

Figure 2 shows representative cross-sections of the samples with 0.5 and 0.2 mm diameter cavities after 20 hours of  $\text{CO}_2$  exposure. In addition to the carbonation of the bulk cement, calcium carbonate was found to precipitate in the microcavities. Calcium carbonate formed also in the cement matrix giving rise to increased material density and thus enhanced X-ray absorption manifested in the  $\mu$ -CT images as increased brightness. The brighter zones in the  $\mu$ -CT images were identified as the carbonation zone. Within the carbonation zone the dissolved portlandite is being precipitated as calcium carbonate in the cement micrometer size pores (being below the resolution of the experiment). In the case of the sample with a 0.5 mm cavity the carbonated zone progressing from the external sample surface was on average thicker than the zone progressing from the void surface. This observation suggests that the carbonation processes are faster nearby the external sample surface. Similar observations were made for the sample with 0.2 mm cavity although the carbonation of this sample was less than for the 0.5 mm cavity sample, possibly suggesting that the cement in this sample had a different porosity.

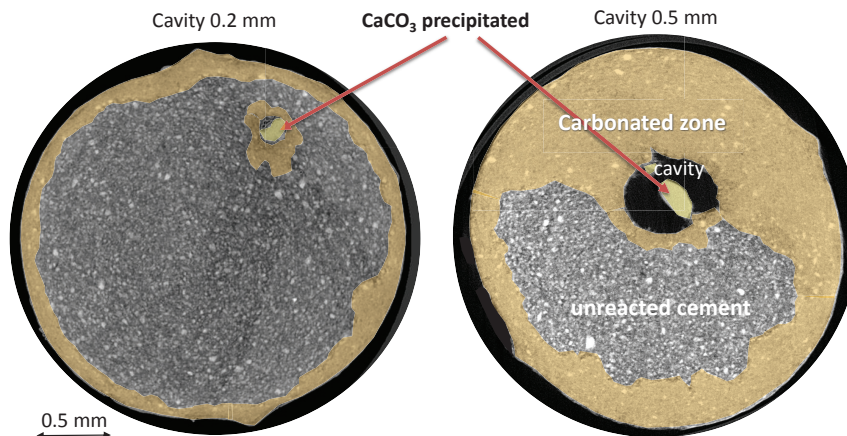


Fig. 2. Horizontal cross sections ( $\mu$ -CT) of the cement samples with 0.2 and 0.5 mm void after 20 hours of exposure to  $\text{CO}_2$  saturated brine.

The CO<sub>2</sub> exposed samples were further imaged by using a scanning electron microscope (SEM) equipped with a backscattered electron (BSE) detector. The SEM-BSE image obtained for the sample with 0.5 mm void is presented in Figure 3. The four regions characteristic for carbonated cement have been distinguished according to Kutchko et al.[2]: I) unreacted cement, II) Ca(OH)<sub>2</sub> depleted zone, III) fully carbonated zone and IV) calcium carbonate depleted zone.

The unhydrated cement grains in zone I appeared as the brightest spots with well-defined boundaries. Pores and silica gel appeared as the darkest spots and could be well distinguished within zone IV. The portlandite (Ca(OH)<sub>2</sub>) and calcium-silicate-hydrate (C-S-H) phases having an intermediate brightness were seen as regions with diffuse outlines rather than well-defined grains and can be observed in regions I and II. Calcium carbonate appeared in zone III as the regions filling up the space between the darkest and the brightest spots, which are pores/silica gel and unhydrated grains, respectively.

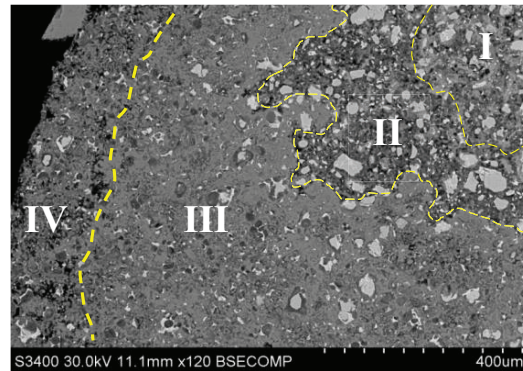


Fig 3. a) SEM-BSE image of cement with 0.5 mm cavity exposed for 20 hours to CO<sub>2</sub> showing the different carbonation zones: I- unreacted cement; II - C-H depleted zone; III- carbonated zone; IV- CaCO<sub>3</sub> dissolution zone.

Chemical numerical simulations were performed in order to conceptually understand the observed differences in the dissolution and precipitation profiles within the cement surrounding the cavity compared to the regions nearby the external surfaces of the cement sample. The differences might have resulted from different availability of CO<sub>2</sub> in the system. To test this hypothesis, two types of models were established: the *open* and *closed* system with respect to CO<sub>2</sub> supply to the cement. Fig. 4 shows a schematic representation of the two models used. In the closed system, all cells are initially in the equilibrium with the CO<sub>2</sub> at 50 bars but a limited amount of CO<sub>2</sub> is available. In the open system, the amount of available CO<sub>2</sub> was unlimited and all cells in water were in equilibrium with CO<sub>2</sub> at 50 bar. Changes in the composition within both aqueous and cement phases after 275 min of reaction were calculated. The data are presented in Figure 5.

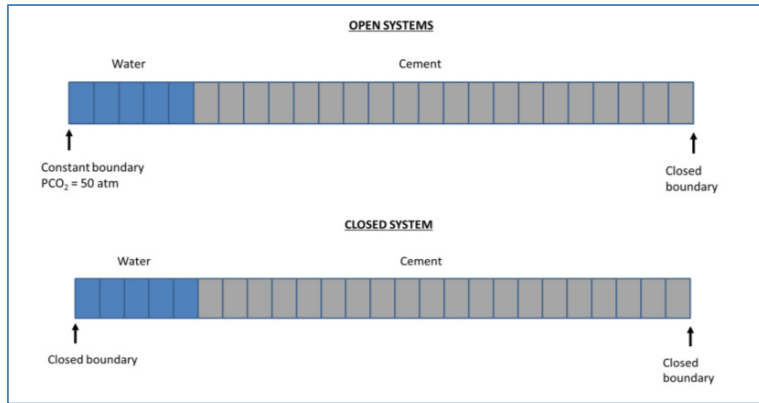


Fig.4. Schematic illustration of the two system models: *open* and *closed*

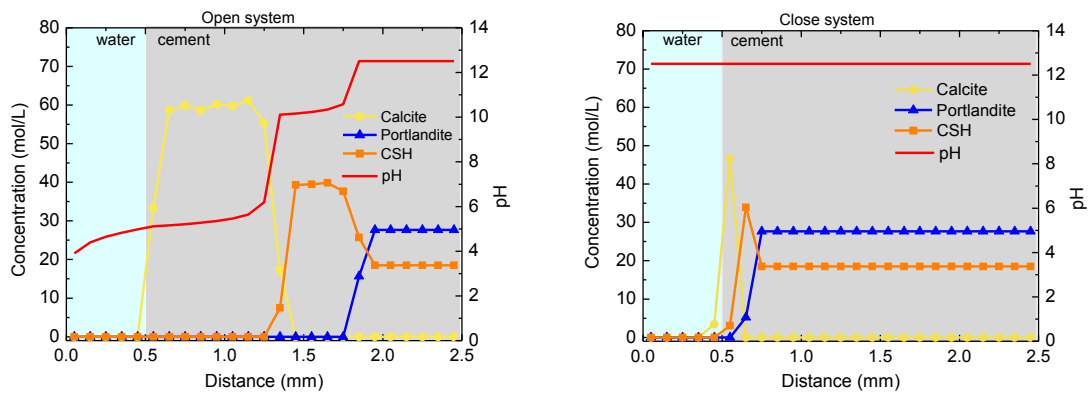


Fig. 5. Calcite, Portlandite and C-S-H concentration variations along the solution and the cement interface for a) open and b) closed system after 275 min of reaction.

The open system model showed that after 275 minutes of reaction with constant  $\text{CO}_2$  supply three regions in the cement matrix can be distinguished, cf. Fig. 5. The region nearest to the water/cement interface was most abundant with calcite. This region was approximately 0.8 mm thick and was depleted from C-S-H and portlandite. The second region ranging between 0.8 and 1.5 mm from the water/cement interface was most abundant in C-S-H and depleted from portlandite. In the third region located deeper than 1.5 mm from the interface portlandite was the most abundant phase. However, no or very little precipitation of calcite in the water cells was observed. pH in the water surrounding the cement was around 4-5 and increases gradually inside the cement, i.e. in the calcite-rich region pH was around 6 and increased further to approximately 10 in the C-S-H rich region. In the region dominated by portlandite and unaffected by reaction with  $\text{CO}_2$ , the pH is approximately 12.5.

Similarly, the results from the closed system model also showed the expected sequence of minerals near the interface, namely, calcite, C-S-H, portlandite, but the calcite and C-S-H rich regions were much narrower compared to the results obtained with the open system. The unaffected portlandite rich region started already from a depth of

0.25 mm from the interface. The pH in the closed system after 275 minutes of reaction was constant around 12.5 throughout the entire system. In this system calcite precipitated also in the water phase.

The carbonation processes have previously been suggested by Kutchko et al. to proceed by following mechanisms[2]. First the carbon dioxide dissolves in water and reacts with water to form carbonic acid. This results in lowering the pH of the solution. When this acidic solution containing carbonic acid diffuses into the cement matrix, the dissociated acid reacts with portlandite and C-S-H. As a result of these reactions calcium carbonate precipitates inside the cement matrix. It has been shown that calcium carbonate can also precipitate inside defects such as voids, cracks, pores etc. and thus result in a decrease of cement porosity and permeability[8,17]. This effect has been referred to in the literature as self-sealing or self-healing[6].

In our experiments the self-healing process led to partial sealing of artificially made voids. After 20 h of CO<sub>2</sub> exposure, 22 and 40 % of the 0.5 and 0.2 mm diameter cavities were filled by precipitated calcite, respectively. If there were enough portlandite and C-S-H in the cement matrix and there were an unlimited CO<sub>2</sub> supply, we estimate that the 0.5 and 0.2 mm cavities would have been sealed after 3.8 and 2 days, respectively. Calcium carbonate precipitated not only inside the voids but also in the cement bulk. It has been observed both as a brighter zone in  $\mu$ -CT scans as well as in the SEM-BSE images (zone III, Fig. 3). Importantly, no precipitation was observed neither in the solution surrounding the cement sample nor at the external sample surfaces, see Fig. 2. In order to understand why the calcite precipitates only in the voids but not at the external sample surfaces, conceptual numerical simulations were performed. In case of an open system, where CO<sub>2</sub> supply is constant and unlimited, the pH in the solution surrounding the cement sample is kept low (see Fig. 5a, red line). The low pH does not support calcite precipitation but rather the dissolution of calcite[18]. The numerical simulation results confirm that no or very little calcium carbonate precipitate is present in the solution at cement sample surfaces in the case where CO<sub>2</sub> supply is unlimited (Fig. 5a, yellow line). Contrary to this, some precipitation of calcite in the aqueous solution occurs close to the water/cement interface in the case with closed system boundary conditions. The main reason for this is that the limited supply of CO<sub>2</sub> enables a much higher pH of 12.5 in the entire water/cement system. At this pH, the activity of the CO<sub>3</sub><sup>2-</sup> ion is much higher relative to the open boundary system, and therefore calcite precipitation takes place at much lower Ca<sup>2+</sup> concentrations. Thus, calcium ions released inside the cement due to dissolution of portlandite and C-S-H will in both cases diffuse back into the water, but while low pH in the open boundary case prevents the calcium ions from precipitating as calcite, the high pH in the closed boundary system results in calcite precipitation near the interface[18].

The experimental conditions at the external sample surfaces and in the surrounding solution, with unlimited availability of CO<sub>2</sub>, correspond to the *open* model system. On the other hand inside the void the availability of CO<sub>2</sub> is limited by the diffusion along the length of the void. This system thus resembles more the closed system although it is not an ideal closed system because CO<sub>2</sub> can be constantly supplied to the void, however with a significantly reduced rate compared with at the external surfaces. This mechanism also provides a possible explanation why the carbonated layer near the external surfaces was observed to be thicker than the thickness of the carbonated layer around the void. In case of limitations of mass exchange the carbonation process goes more slowly and is more prone to provide self-healing. The limitations of CO<sub>2</sub> supply can be either geometrical or flow dependent. Brunet et al. have made a study to identify key controlling parameters and offer general guidelines to predict when self-sealing occurs[19]. Their focus was on reactive transport rather than static carbonation conditions but they have also identified that the interplay between the two parameters fracture volume and the flow rate of the brine drives either sealing or opening of the existing voids/fractures. Based on their studies and the results presented here, we conclude that both under static and flow conditions both fracture geometry and mass transport associated with flow rate (under flow conditions) or diffusive transport (under static conditions) are the parameters that determine whether self-healing will occur or not.

#### 4. Conclusions

Carbonation of well cement has been investigated using X-ray computed micro-tomography, BSE-SEM and chemical reaction simulations. The cured Portland G well cement sample was exposed to CO<sub>2</sub> saturated brine at 100 bars at room temperature. The samples had artificially made cylindrical cavities with a diameter of 0.5 and 0.2 mm. The carbonation processes included self-healing of the voids, carbonation of the bulk cement and leaching of CaCO<sub>3</sub>. It was shown that at batch conditions CaCO<sub>3</sub> precipitated in the voids leading to partial sealing of the cavities. Simulations were performed to quantify the differences in carbonation under conditions of ample or no CO<sub>2</sub> supply. It has been shown that in open systems where CO<sub>2</sub> supply is quick and unlimited, calcium carbonate precipitation is unlikely. On the other hand if CO<sub>2</sub> transport is limited by e.g. slow diffusion in a static system, calcium carbonate precipitation was likely to occur. The effect was found to be closely related with pH changes that are associated with carbonic acid consumption. Self-healing of defects inside the well is promoted in the case of impeded CO<sub>2</sub> supply, while in the case of unlimited CO<sub>2</sub> availability leaching of the cement is more probable.

#### Acknowledgements

This study has been carried out through the projects "Closing the gaps in CO<sub>2</sub> well plugging" and "Ensuring well integrity during CO<sub>2</sub> injection" funded by the Research Council of Norway (243765/E20). These projects are administered as an integrated part of the BIGCCS Centre funded by Gassco, Shell, Statoil, Total, Engie and the Research Council of Norway (193816/S60). The Research Council of Norway funded the tomography equipment through the National Research Centre for X-ray Scattering and Imaging (RECX). H.O.S. and Y.Y. acknowledge support from Innovation Fund Denmark via the CINEMA project and the European Union's Horizon 2020 research and innovation programme under the Marie Skłodowska-Curie grant agreement No 653241. Partial funding for this work was obtained from the Norwegian PhD Network on Nanotechnology for Microsystems, which is sponsored by the Research Council of Norway, Division for Science, under contract no. 221860/F40.

#### References

- [1] IPCC Special report on Carbon Dioxide Capture and Storage, B. Metz, 2005.
- [2] Kutchko B, Strazisar BR, Dzombak D, Lowry GV, Thaulow N. Degradation of Well Cement by CO<sub>2</sub> under Geologic Sequestration Conditions. *Environ. Sci. Technol.* 2007;41: 4787–4792.
- [3] Mason HE, Du Frane WL, Walsh SDC, Dai Z, Charnvanichborikarn S, Carroll SA. Chemical and Mechanical Properties of Wellbore Cement Altered by CO<sub>2</sub>-Rich Brine Using a Multianalytical Approach. *Environ. Sci. Technol.* 2013;47: 1745–1752.
- [4] Kjølner C, Sigalas L, Frykman P, Bjørge R, Torsæter M. Cement Self-Healing as a Result of CO<sub>2</sub> Leakage. *Energy Procedia.* 2016;86:342–351.
- [5] Zhang M, Bachu S. Review of integrity of existing wells in relation to CO<sub>2</sub> geological storage: What do we know?. *Int. J. Greenh. Gas Control.* 2011;5: 826–840.
- [6] Liteanu E, Spiers CJ. Fracture healing and transport properties of wellbore cement in the presence of supercritical CO<sub>2</sub>. *Chem. Geol.* 2011;281: 195–210.
- [7] Wigand M, Kaszuba JP, Carey JW, Hollis WK. Geochemical effects of CO<sub>2</sub> sequestration on fractured wellbore cement at the cement/caprock interface. *Chem. Geol.* 2009;265:122–133.
- [8] Bachu S, Bennion DB. Experimental assessment of brine and/or CO<sub>2</sub> leakage through well cements at reservoir conditions. *Int. J. Greenh. Gas Control.* 2009;3:494–501.
- [9] Abdoulghafour H, Luquot L, Gouze P. Characterization of the Mechanisms Controlling the Permeability Changes of Fractured Cements Flowed Through by CO<sub>2</sub>-Rich Brine. *Environ. Sci. Technol.* 2013;47: 10332–10338.
- [10] Luquot L, Abdoulghafour H, Gouze P. Hydro-dynamically controlled alteration of fractured Portland cements flowed by CO<sub>2</sub>-rich brine. *Int. J. Greenh. Gas Control.* 2013;16: 167–179.
- [11] Standard 10 B-2, (API), American Petroleum Institute.
- [12] Schneider CA, Rasband WS, Eliceiri KW. NIH Image to ImageJ: 25 years of image analysis, *Nat. Methods.* 2012;9:671–675.
- [13] Parkhurst DL, Appelo CA. User's guide to PHREEQC (Version 2)—A computer program for speciation, batch-reaction, one-dimensional transport, and inverse geochemical calculations: U.S. Geological Survey Water-Resources Investigations Report 1999: 99–4259.
- [14] Blanc P, Lassin A, Piantone P, Azaroual M, Jacquemet N, Fabbri A, Gaucher EC, Thermodem : A geochemical database focused on low temperature water/rock interactions and waste materials. *Appl. Geochemistry.* 2012;27: 2107–2116.



- [15] Cadogan SP, Hallett JP, Maitland C, Trusler JPM. Diffusion Coefficients of Carbon Dioxide in Brines Measured Using  $^{13}\text{C}$  Pulsed-Field Gradient Nuclear Magnetic Resonance. *J. Chem. Eng. Data*. 2015;184:15–18.
- [16] Soive A, Roziere E, Loukili A. Parametrical study of the cementitious materials degradation under external sulfate attack through numerical modeling. *Constr. Build. Mater*. 2016;112: 267–275.
- [17] Garcia-Gonzalez CA, el Grouh N, Hidalgo A, Fraile J, Lopez-Periago AM, Andrade C, Domingo C. New insights on the use of supercritical carbon dioxide for the accelerated carbonation of cement pastes. *J. Supercrit. Fluids*. 2008;43:500–509.
- [18] Thaulow N, Lee RJ, Wagner K, Sahu S. Effect of calcium hydroxide on the form, extent, and significance of carbonation. In: Skalny JP, Gebauer J, Odler I, editors. *Calcium Hydroxide Concr.*, The American Ceramic Society. Westerville: Ohio: 2001: p. 191–201.
- [19] Brunet JPL, Li L, Karpyn ZT, Huerta NJ. Fracture opening or self-sealing: Critical residence time as a unifying parameter for cement– $\text{CO}_2$ –brine interactions. *Int. J. Greenh. Gas Control*. 2016;47: 25–37.